



HAL
open science

The Sugetbrak basalts from northwestern Tarim Block of northwest China: Geochronology, geochemistry and implications for Rodinia breakup and ice age in the Late Neoproterozoic

Bei Xu, Haibo Zou, Yan Chen, Jinyou He, Yu Wang

► To cite this version:

Bei Xu, Haibo Zou, Yan Chen, Jinyou He, Yu Wang. The Sugetbrak basalts from northwestern Tarim Block of northwest China: Geochronology, geochemistry and implications for Rodinia breakup and ice age in the Late Neoproterozoic. *Precambrian Research*, 2013, 236, pp.214-226. <10.1016/j.precamres.2013.07.009>. <insu-00859605>

HAL Id: insu-00859605

<https://insu.hal.science/insu-00859605v1>

Submitted on 29 Oct 2013

HAL is a multi-disciplinary open access archive for the deposit and dissemination of scientific research documents, whether they are published or not. The documents may come from teaching and research institutions in France or abroad, or from public or private research centers.

L'archive ouverte pluridisciplinaire **HAL**, est destinée au dépôt et à la diffusion de documents scientifiques de niveau recherche, publiés ou non, émanant des établissements d'enseignement et de recherche français ou étrangers, des laboratoires publics ou privés.



HAL Authorization

The Sugetbrak basalts from northwestern Tarim Block of northwest China: Geochronology, geochemistry and implications for Rodinia breakup and ice age in the Late Neoproterozoic

Bei Xu^{a,*}, Haibo Zou^b, Yan Chen^c, Jinyou He^d, Yu Wang^a

^a*Key Laboratory of Orogenic Belts and Crustal Evolution, Ministry of Education, Peking University, Beijing, 100871, China*

^b*Department of Geology and Geography, Auburn University, Auburn, AL 36849, USA*

^c*ISTO, Department of Geosciences, Orleans University, Orleans, 45067, France*

^d*China University of Geosciences, Beijing, 100083, China*

*Corresponding author E-mail address: bxu@pku.edu.cn (Bei Xu)

Corresponding address: Department of Geology, Peking University, Beijing 100871, China

Abstract

Zircons from two samples of the Sugetbrak basalts (SB) yield weighted mean ages of 615.2 ± 4.8 Ma and 614.4 ± 9.1 Ma. These ages, interpreted as the eruption age of the SB, provide an age constraint on the timing of the Sugetbrak Formation in Sugetbrak, northwestern Tarim Block, China. These two ages suggest that the igneous activities related to the breakup of the Neoproterozoic supercontinent Rodinia lasted until 614–615 Ma in at least the northwest Tarim Block. Geochemical analysis indicates that the SB was generated in an intra-continental rifting environment. Application of the dynamic melting inversion method suggests that the Sugetbrak basalts represent 7–12% partial melts. Unlike large-volume tholeiites, these low-degree transitional basaltic melts may represent the waning stage of plume volcanism during a long-lasting continental breakup. Based on the ages of the SB and its stratigraphic relationship with the Yuermeinak diamictite, the Yuermeinak glaciation in the Sugetbrak section of the northwest Tarim Block should correlate with the Tereekeng glaciation in the Qurugtagh area of the northeast Tarim Block, the Nantuo glaciation in Yangtze Block, and the Elatina glaciation in South Australia.

Keywords: Late Neoproterozoic, Tarim Block, Rodinia, SHRIMP U-Pb age, Glaciation

1. Introduction

Magmatic rocks associated with the Rodinia breakup may record critical information on the timing and processes of continental breakup, as they can be precisely dated, and provide clues regarding crustal thickness and mantle sources (Kullerud et al., 2006). The Neoproterozoic breakup of the Rodinia supercontinent has attracted much attention recently

(Jefferson, et al., 1989; Li, et al., 1996; Veevers, et al., 1997; Wingate, et al., 1998; Li, 1999, Karlstrom, et al., 2000; Veevers, 2000; Li and Powell, 2001; Dieren, et al., 2003; Li, et al., 2003; 2006; Kheraskova, et al., 2010). This event, developed in Australia, East Antarctica, Yangtze, and the Tarim Block, is divided into four stages in the Tarim Block: 820-800 Ma, 780-760 Ma, 740-735 Ma and 650-635 Ma (Li, et al., 1996; 2001; 2003; 2008; Li, et al., 2010; Zhang, et al., 2011; Zhang, et al., 2012). The ages of these magmatic events have been employed to constrain the division of the Neoproterozoic ages (Ross and Villeneuve, 1997; Hoffman and Schrag, 2002; Hoffmann, et al., 2004; 2006; Zhou, et al., 2004; Condon, et al., 2005; Zhang, et al., 2005; Xu et al., 2009; Macdonald, et al., 2010).

The Tarim Block has Neoproterozoic magmatic records similar to those of the Yangtze Block, and may have been located on the periphery of the proposed Rodinia superplume (Li Z.X. et al., 1999; Chen et al., 2004; Xu et al., 2005, 2009; Zhang et al., 2009; Lu et al., 2008; Shu et al., 2011). Four stages of Neoproterozoic magmatic events have been reported in the Tarim Block. The first two (820-800 Ma and 780-760 Ma) stages, represented by ultramafic-mafic complexes, adakitic granites, and mafic dykes, are interpreted to be a result of the partial melting of thickened lower crust triggered by underplating of a Rodinian superplume (Long, et al., 2011; Zhang, et al., 2009; 2011a; 2011b). The third (740-735 Ma) stage, consisting of bimodal volcanic rocks and the fourth (650-635 Ma) stage, composed of mafic dykes, potassic granitoids, peraluminous granite and volcanic rocks, are attributed to rifting in the Tarim Block (Xu, et al., 2005; 2009; Zhang et al., 2011; Zhu, et al., 2011). However, the presence of 615 ± 15 Ma volcanic rocks in the Mochia-Khutuk area of the northeast Tarim Block (Xu, et al., 2009), and 588-619 Ma detrital zircons in the Aksu area of the northwest Tarim Block (Zhu, et al.,

2011), may indicate that there was a magmatic event even younger than the fourth event. This is useful for investigating the waning stage of the Rodinia superplume breakup in the Tarim Block.

In this paper we report new ages of basalts from the Neoproterozoic Sugetbrak Formation in the Sugetbrak section of the Aksu area, NW Tarim Block, and discuss their tectonic implications for the glaciation correlation and intra-continental rifting in the Late Neoproterozoic.

2. Geological setting

2.1. Neoproterozoic strata in the Aksu area of the northwest Tarim Block

Neoproterozoic strata occur in the Aksu area of northwest Tarim, the Quruqtagh area of northeast Tarim, and the Yecheng area of southwest Tarim. Strata containing volcanics have been found from the Aksu area and the Quruqtagh area (Gao and Zhu, 1984; Xu et al., 2005; Wang et al., 2010a, Fig. 1B).

In the Aksu area, the Neoproterozoic strata crop out in southwest Aksu, Wushi and Sugetbrak (Fig. 1C). In the sections of southwest Aksu and Wushi, the strata include the Aksu Group and the overlying Sugetbrak and Chigebrak Formations. The Aksu Group is composed of pelitic, psammitic, and mafic schists. Mafic schists are characterized by greenschists and blueschists that are considered to be some of the oldest high-pressure metamorphic rocks (Liou et al., 1989, 1990; 1996; Nakajima et al., 1990; Zhang, et al., 1999). A tectonic evolution model for the Aksu blueschist has been proposed (Zhang, et al., 2010; Zhu et al., 2011). There is a clear angular unconformity between the Aksu Group and the overlying Sugetbrak Formation in southwest Aksu and Wushi (Gao, et al., 1985; Turner, 2010; Zhu, et al., 2011). The 400-450 m thick Sugetbrak

Formation is composed of red conglomerates, red fluvial sandstones and grey lacustrine mudstones with three horizons of basalts. The Chigebrak Formation is characterized by thick dolostone and is overlain unconformably by the Cambrian Yuertus Formation (Gao et al., 1986; Turner, 2010; Zhu et al., 2011).

In the Sugetbrak section, the Neoproterozoic shows a different succession composed of, from bottom to top, the Qiaoenbrak, Yuermeinak, Sugetbrak and Chigebrak Formations (Fig. 2A, 2B). The Qiaoenbrak Formation is composed of epimetamorphic sandstone and siltstone flysch, with a thickness of 1966-2094 m (Gao, et al., 1986). The glacial origin of this formation is debated. For example, Gao et al. (1993) suggested that it is part of a turbidite sequence. It is unconformably overlain by the Yuermeinak Formation and is considered to be marine glacier deposits due to the presence of several interbedded diamictites (Gao, et al., 1986). The Yuermeinak Formation occurs only in the Sugetbrak area, and is characterized by diamictites up to 61 m thick, which are interpreted to be continental glacier deposits (Gao, et al., 1986). The Sugetbrak Formation can be divided into the Lower and Upper members in Sugetbrak (Fig. 2B, 2C; Gao, et al., 1986; Zhan, et al., 2007). The Lower Sugetbrak Formation (108-461 m) is composed of thin-layered red sandstone, quartz sandstone, siltstone and mudstone with a discontinuous horizon of 5-10 m thick basalt in its lower part, followed by 79 m thick volcanic rock above (Fig. 2C). The Upper Sugetbrak Formation conformably overlies the Lower member and is conformably overlain by the Chigebrak Formation. The Upper Sugetbrak Formation comprises 82 m thick red and grey thin-layered sandstone and mudstones with interbedded limestones (Fig. 2B, Gao, et al., 1986).

Fig. 1.(A):Tectonic location of Tarim Block in China;(B):Geological map of Tarim Block, West

China; (C): Geological map of the Aksu area

Fig. 2. (A): Geological map of the Sugetbrak section and sample positions; (B): the Neoproterozoic stratigraphic column in Sugetbrak; (C): photos of the Neoproterozoic strata in Sugetbrak

2.2. Sugetbrak basalt (SB) and samples

The Sugetbrak basalt (SB) occurs in southwest Aksu, Wushi and Sugetbrak in the Aksu area (Fig. 1C) of the northwest Tarim block. There are between 2 and 4 horizons of this basalt in the southwest Aksu section, with thicknesses of 15-30 m (Wang, et al., 2010a; Zhu, et al., 2011). Two 4-5 m thick horizons of the SB are also reported in the Wushi section 45 km to the northwest (Turner, 2010). In the Sugetbrak section, the SB is much thicker and has repeated occurrences caused by an E-W extending syncline. On the north limb of the syncline, a 79 m thick SB occurrence crops out at the top of the Lower member of the Sugetbrak Fm. (Fig. 2B, 2C) and shows conformity relationships with the underlying sandstone (Fig. 3A), where 7 samples of A group (05822, Y1, Y2, Y5, Y6, Y7 and Y8; Fig. 2A) were collected. A discontinuous horizon of 5-10 m thick columnar-jointed basalt (Fig. 3B) occurs in the middle of the Lower member of the Sugetbrak Fm. (Fig. 2B, 2C), showing a conformity relationship with underlying sandstones. On the south limb of the syncline, a continuous horizon of the SB, characterized by pillow lava, (Fig. 3D) extends for several kilometers (Fig. 3C), and shows a conformity relationship with overlying red sandstones (Fig. 3E). Here, 9 samples of B group (05823, 830S2, 831S51, 83156, 83158, 83160, 83161, 83163 and 831S81) were collected (Fig. 2A). These columnar jointed basalts and pillow lava in the SB, combined with sedimentary structures, such as large herringbone (Fig. 3A) and ripple bedding (Fig. 3F) in the red sandstones, suggest a very shallow continental sedimentary environment during the period of SB magmatism. About 4 km southwest of Sugetbrak, two basaltic

flows have been reported (Zhang, et al., 2012).

Fig.3. Photographs of the SB and sedimentary rocks of the Sugetbrak Formation.

2.3. Previous geochronology for the SB

Seventeen zircons from the SB from southwest Aksu have been dated by the LA-ICP-MS method and yielded three ages of 1926 ± 27 Ma, 1432 ± 22 Ma and 807 ± 21 Ma. These ages have been interpreted as the ages of Mesoproterozoic metamorphic zircons and Late Neoproterozoic inherited magmatic zircons (Wang et al., 2010a). The youngest age in these inherited zircons is 755 Ma, suggesting that the SB is younger than 755 Ma (Wang, et al., 2010a). Recently, Zhang et al. (2012) reported a LA-ICP-MS U-Pb age of 783.7 ± 2.3 Ma from the SB, about 4 km southwest of Sugetbrak, and interpreted this age as the crystallization age of the SB.

3. Analytical procedures

Two samples from the SB, 05822 and 05823, were analyzed by the SHRIMP U-Pb method for age dating. In addition, these two samples and the 14 other SB samples were analyzed to determine their major and trace elements compositions.

Zircons for SHRIMP analyses were separated from samples 05822 and 05823 in the SB according to magnetic properties and density, and purified by hand picking. The zircons, together with several grains of TEMORA, were cast in an epoxy mount and polished down to half section. Cathodoluminescence (CL) imaging was used to guide the SHRIMP analyses. The CL study was undertaken on a FEI-XL30SFEG electron microscope at the Department of Electronics, Peking University.

The SHRIMP U-Pb analyses were performed on the Beijing SHRIMP II at the Chinese Academy of Geological Sciences, Ministry of Land and Resource of Peoples' Republic of China. The analytical procedures followed the methodology of Williams et al (1987) and Compston et al (1992). For the zircon analyses, nine ion species of Zr_2O^+ , $^{204}Pb^+$, $^{207}Pb^+$, $^{206}Pb^+$, $^{208}Pb^+$, U^+ , Th^+ , ThO^+ , UO^+ and background were measured on a single electron multiplier by cyclic stepping of the magnetic field, recording the mean ion counts of every 7 scans. A primary ion beam of c. 4.5 nA, 10 kV O^{-2} and c. 20-25 μm spot diameter was used. Masses were analyzed at a mass resolution of c. 5000 (1% peak height). Inter-element fractionation in the ion emission of zircon was corrected relative to the ANU RSES references, using the TEMORA (417 Ma, $^{206}Pb^*/^{238}U=0.06683$). Errors on individual analysis are at the 1σ level based on counting statistics. The reproducibility of TEMORA was repeatedly measured at c. 3%. The software of Ludwig SQUID 1.0 and attached ISOPLOT were used for data processing (Ludwig, 1999; 2001). The ages were calculated using the decay constants recommended by IUGS (1977). The weighted mean ages were quoted at a 95% confidence level. The initial lead component was corrected using measured ^{204}Pb .

Major element oxides were determined by x-ray fluorescence using glass disks at the Laboratory of Orogenic Belts and Crustal Evolution, Ministry of Education, Peking University. Analytical precision as determined on duplicate analyses was generally around 1–5%. For trace element analyses, about 50 mg sample powders were dissolved using a $HF+HNO_3$ mixture in a Teflon bomb at $\sim 190^\circ C$ for 48 h. Trace elements were analyzed using a Finnigan Element IIICP-MS at the Center of Modern Analysis, Nanjing University. Analytical precision for trace elements was better than 5%. Detailed analytical procedure followed Gao et al. (2003).

4. U-Pb zircon geochronology

The measured isotopic ratios and calculated ages for samples 05822 and 05823 are given in Table 1 and illustrated on Concordia plots in Fig. 4B. The measured U concentrations for these zircon grains vary from 960 to 58 ppm; Th, from 949 to 63 ppm; and Th/U ratios, from 1.59 to 0.26, which suggests that all zircons belong to a magmatic type.

Twenty-nine zircons were dated in total, and can be divided into three groups (Table 1). Zircons of group 1 are ~150 μm in size, show weakly zoned textures (Fig. 4A, 05823-11-4.1), and yield a $^{207}\text{Pb}/^{206}\text{Pb}$ age of 1756 ± 9 Ma (Table 1, 05823-11-4.1), indicating the Mesoproterozoic magmatism (Hu, et al., 2000). Most zircons of groups 2 and 3 are smaller, ranging from 80 to 30 μm . They are euhedral with oscillatory zoning, indicative of magmatic zircons (Fig. 4A). $^{206}\text{Pb}/^{238}\text{U}$ ages of twenty-four zircons of group 2 range from 676 to 864 Ma, and form several intervals of 676-691 Ma (n=3), 707-743 Ma (n=5), 751-790 Ma (n=7) and 806-864 Ma (n=9, Table 1). These ages represent inherited zircon ages and reflect multiple magmatic episodes related to Rodinia breakup in the Late Neoproterozoic (Zhang, et al., 2011b; Zhu et al., 2011b; Wang, et al., 2010a). Interestingly, there are four zircons in group 3 that yield $^{206}\text{Pb}/^{238}\text{U}$ ages from 617 to 612 Ma (05822-1-7.1, 05822-1A-5.1, 05823-11-2.1 and 05823-11-5.1), which give two concordia ages of 615.2 ± 4.8 Ma (Fig. 4B) for sample 05822 and 614.4 ± 9.1 Ma (Fig. 4C) for sample 05823. Because these 4 youngest zircons are euhedral and the smallest in size, their concordia ages of 614-615 Ma are interpreted as the eruption age of the SB, although we cannot completely rule out the possibility that the ~615 Ma zircons may represent the youngest inherited zircons. In the case of youngest zircon inheritance, the eruption age of the Sugetbrak basalts would be slightly

younger than ~615 Ma.

Table 1. Zircon U-Pb isotopic data

Fig. 4. Cathodoluminescence images and Zircon concordia plots

5. Geochemistry

Major and trace elements of the SB are listed in Table 2. They are characterized by high TiO_2 contents (2.2-4.0%). Their Al_2O_3 ranges from 13.9% to 17.7%. Total alkali content ranges from 2.9% to 5.4%, with $\text{Na}_2\text{O} > \text{K}_2\text{O}$. Their high LOI contents, ranging from 2.7% to 8.7%, indicate alterations. Na_2O and K_2O were probably mobile during alterations, and thus cannot be employed for rock classifications using the total alkali vs. silica diagram.

Table 2. Major and trace elements of the SB

Petrologically, it is useful to determine whether the rocks are alkali basalts or tholeiites. Here we use immobile trace elements such as Nb and Y to further evaluate their alkali character. These samples have Nb/Y ratios ranging mostly from 0.58 to 0.68. In the $\text{Zr}/\text{TiO}_2 - \text{Nb}/\text{Y}$ diagram (Winchester and Floyd, 1977), they plot on the boundary line between sub-alkaline basalts and alkali basalts (Fig. 7A). In the $\text{Nb}/\text{Y} - \text{Zr}/(\text{P}_2\text{O}_5 * 10000)$ diagram, they also plot near the boundary line between alkali basalts and tholeiitic basalts (Fig. 7B). We thus regard them as transitional basalts.

Fig. 5. A: $\text{Zr}/\text{TiO}_2 - \text{Nb}/\text{Y}$ diagram (Winchester and Floyd, 1977)

B: $\text{Nb}/\text{Y} - \text{Zr}/(\text{P}_2\text{O}_5 * 10000)$ diagram (Floyd and Winchester, 1975)

All samples are enriched in light rare earth elements (LREEs, Fig. 6A). They lack negative Eu anomalies, indicating that plagioclase is not a fractionating phase. In the Spider diagram (Fig.

6B), they display positive anomalies in Ba and Pb and negative anomalies in Rb and Sr. They do not show negative Nb anomalies.

Fig. 6.A: REE diagram; B: Spider diagram

6. Discussion

6.1 Petrogenesis and tectonic settings

6.1.1 Within-plate environments

Ti, Zr, Y and Nb are immobile trace elements during zeolite to greenschist facies metamorphism, and may be useful for the determination of tectonic environments of basaltic rocks (Pearce and Cann, 1973; Winchester and Floyd, 1975). In the Ti-Zr-Y diagram (Pearce and Cann, 1973), the lavas plot in the “within-plate” basalt field (Fig. 7A). In the Nb-Zr-Y diagram (Meschede, 1986), the samples plot on the boundary line between fields AII and C, indicating an intraplate tectonic setting (Fig. 7B). The boundary line is the transition between intraplate alkali basalts and intraplate tholeiites. Both Ti-Zr-Y and Nb-Zr-Y diagrams suggest a within-plate environment, ruling out the possibility of a volcanic arc or ocean-ridge environment. The lack of any negative Nb anomaly in the spider diagram also argues against the island arc or continental arc environment. Therefore, the SB are intra-continental transitional basalts. Our inference of a within-plate (intra-continental) tectonic setting for the SB is largely consistent with the work by Zhang et al. (2012).

Fig. 7. A: Ti-Zr-Y diagram (Pearce and Cann, 1973);

B: Nb-Zr-Y diagram (Meschede, 1986)

6.1.2. Low-degree small-volume melts

The high Ti contents in all samples reflect low degree partial melts. We have used the dynamic melting inversion (DMI) method (Zou and Zindler, 1996; Zou, 1998; Zou et al., 2000) to estimate the degrees of partial melting more quantitatively. The DMI method uses variations of between-magma concentration ratios for two incompatible elements with different partition coefficients, and does not require assumptions about mantle rock concentrations or ratios. Two immobile trace elements are selected with different partition coefficients, Nb and Zr. Note that Nb is more incompatible than Zr. The concentration ratios between a low-degree melt sample (sample 831S41) and a high-degree melt sample (sample 83161) are 1.51 ($=24.63/16.27$) for Nb and 1.31 ($=200/152$) for Zr. Samples 831S41 and 83161 are selected because sample 831S41 has the highest incompatible element concentrations (representing the lowest degree of partial melting) while sample 83161 has the lowest incompatible element concentrations (indicative of the highest degree of melting) in B Group. The degree of partial melting calculated using DMI by solving a system of simultaneous non-linear equations is 7.4% for sample 831S41, and 10.9% for sample 83161, using bulk partition coefficients of 0.01 for Nb and 0.04 for Zr. If we still select sample 831S41 as a low-degree melt, but select another sample such as 83160 as a high-degree melt (another sample with low incompatible element concentrations in B Group), then the low-degree/high-degree concentration ratios are 1.52 ($=24.63/16.27$) for Nb and 1.33 ($=200/150$) for Zr, and the partial melting degrees using DMI are 7.9% for sample 831S41 and 11.8% for sample 83160. Thus, these transitional basalts were produced at 7-12% mantle partial melting.

Note that in the calculations we use concentration ratios instead of elemental abundances, because concentration ratios are insensitive to subsequent fractional crystallizations.

Unlike large-volume tholeiites produced in the main stage of plume volcanism, these low-degree, small-volume melts might represent melts formed at the onset stage or the waning stage of a plume during continental breakup. We prefer to consider waning stage of plume volcanism for the creation of the SB because of its younger age, while Zhang et al. (2012) prefer the onset stage of plume volcanism, owing to the different age results for the SB (784 Ma in Zhang et al. (2012) vs. 614-615 Ma from this study). As mentioned above, we regard the 784 Ma age as the age for inherited zircons (see discussion in section 6.2).

6.2. Implications for the rift succession of the Sugetbrak Formation and Neoproterozoic igneous activities

Because the studied samples were collected in the horizons of the SB between the Lower and Upper Sugetbrak members, the new age represents the boundary age between the upper and lower members, further providing a time constraint on the timing of the Sugetbrak Formation in the Sugetbrak section. Recently, the Sugetbrak Formation in the southwest Aksu and Wushi areas has been interpreted as fluvial and lacustrine facies sediments (Turner, 2010; Wang et al., 2010a). Combined with several horizons of basalts that record episodic volcanism, these sedimentary facies are thought to indicate the development of a Neoproterozoic rift system in the Aksu area (Turner, 2010; Wang et al., 2010a). Hence, our new age represents the development age of this rift system in the northwest Tarim Block.

Though four phases of Neoproterozoic igneous activities (820-800Ma, 780-760Ma,

740-735 Ma and 650-635 Ma) have been recognized in the Tarim Block (Zhang et al., 2011), our new age (615 Ma) is even younger, and may represent the last stage of the Neoproterozoic rifting relating to the breakup of the Rodinia Supercontinent in the northwest Tarim Block. It has been noticed that there are simultaneous volcanic rocks in the Qurugtagh area of the northeast Tarim Block, where an age of 615 ± 6 Ma from andesitic lava has been reported (Xu et al., 2009). These data suggest that the igneous activities related to the breakup of the Neoproterozoic Rodinia supercontinent lasted until at least 615 Ma.

Six detrital zircon ages from the red sandstone of the Sugetbrak Formation in southwest Aksu range from 619 to 588 Ma and give a weighted average age of 602 ± 13 Ma (Zhu, et al., 2011), which is younger than the age of the SB from Sugetbrak. The age difference between these places might be due to the fact that the Neoproterozoic succession in southwest Aksu is incomplete, which has been indicated by the lacunas of the Qiaoenbrak and Yuermeinak Formations, and of the bottom part of the Lower Sugetbrak Formation (Fig. 8). Turner (2010) pointed out that small, isolated depocentres and pre-existing topography might cause local variety of basal conglomerates in the Aksu area. Therefore, the age of 602 ± 13 Ma might represent the maximal depositional age of the Upper member of the Sugetbrak Formation (Fig. 9). Obviously, the direct evidence for the age of the Sugetbrak Formation depends on the eruption age of the SB in the southwest Aksu section. According to available geochronological data in the southwest Aksu and Sugetbrak sections, a revised correlation of the Neoproterozoic strata between southwest Aksu, Wushi and Sugetbrak sections is proposed in Fig. 8.

Recently, Zhang et al (2012) reported a LA-ICP-MS U-Pb zircon age of 783.7 ± 2.3 Ma from the SB about 4 km southwest of Sugetbrak, and interpreted it as a crystallization age of the SB. We

regard 784 Ma as the age for inherited zircons instead of the crystallization age for the SB, because the zircons from Zhang et al. (2012) are large crystals (most zircons > 80 μm), similar to group 2 zircons of this study and the inherited zircons of Wang et al. (2010a). In addition, Zhu et al. (2011) have reported several detrital zircon ages ranging from 619 to 588 Ma from the red sandstone of the Upper member of the Sugetbrak Formation, which implies that it is impossible for the Lower member of this formation to be 784 Ma old. Geologically, if this age of 784 Ma is correct, then the underlying Yuermeinak glacier deposits would be older than 784 Ma. However, no Neoproterozoic ice age older than 784 Ma has been reported in the world (Hoffman and Schrag, 2002; Xu, et al., 2009; Macdonald, et al., 2010).

Fig. 8. Correlation of the Neoproterozoic strata between southwest Aksu, Wushi and Sugetbrak areas

6.3. Implications for the correlation of the Yuermeinak glaciation

Ages, distribution, and correlations of the Neoproterozoic glaciations around the world are still controversial (Kaufman et al., 1997; Hoffman et al., 1998; Kennedy et al., 1998; Hoffman and Schrag, 2002; Jiang et al., 2003). Two glaciations (Sturtian and Marinoan, Young, 1995; Kennedy et al., 1998), three glaciations (Sturtian, Marinoan and post-Marinoan, Knoll, 2000, Xiao et al., 2004; Halverson, 2006; McCay et al., 2006) or four glaciations (Kaigas, Sturtian, Marinoan or Elatina and Gaskiers, Hoffman and Schrag, 2002; Hoffmann et al., 2004; Macdonald et al., 2010) have been proposed. On the other hand, four glaciations have been reported in the northeast Tarim Block, including Bayisi (730 Ma), Altungol, Tereeken (725-615 Ma) and Hankalchough

(615-542 Ma) glaciations (Kou et al., 2008; Xu et al., 2008; Xu et al., 2009). However, the age of the Yuermeinak glaciation in the northwest Tarim Block, and its correlation, were previously unknown.

According to the Neoproterozoic succession in the Sugetbrak section (Fig. 9), the Lower member of Sugetbrak Formation containing the SB conformably overlies the Yuermeinak Formation diamictite. Because there is only about 400 m of continental sedimentary succession between the SB and Yuermeinak Formation, the occurrence of the Yuermeinak glaciation is not much earlier than 614-615 Ma. This is similar to the Tereeken glaciation in the Quruqtagh area of the northeast Tarim Block, where there is only the Zhamoketi Formation turbidite between the Tereeken diamictite and volcanic layer with an age of 615 ± 6 Ma (Xu et al., 2009). It is therefore reasonable to correlate the Yuermeinak glaciation with the Tereeken glaciation in the Quruqtagh area. Based on a TIMS U-Pb age of 635.2 ± 0.6 Ma for the Nantuo glaciation (Condon et al., 2005) and an age of 615 ± 6 Ma for the volcanic rocks above the Tereeken glaciation, previous studies have suggested that the Tereeken glaciation can be correlated with the Nantuo glaciation in the Yangtze Block and the Elatina glaciation in Australia (Xu et al., 2009). If this is correct, then the Yuermeinak glaciation should also correlate with them (Fig. 10).

Fig. 10 Correlation of the Neoproterozoic glaciations

7. 8. Conclusion

This study reached the following conclusions:

(1) Small euhedral zircons from two samples of the Sugetbrak basalts (SB) of the Sugetbrak Formation yield weighted mean ages of 615.2 ± 4.8 Ma and 614.4 ± 9.1 Ma. These ages are interpreted

as the eruption age of the SB, thereby providing an age constraint on the timing of the Sugetbrak Formation in Sugetbrak, northwest Tarim Block. These two ages suggest that the igneous activities related to the breakup of the Neoproterozoic Rodinia supercontinent lasted until at least 614-615 Ma in the northwest Tarim Block.

(2) Geochemical analysis indicates that the SB was generated in an intra-continental rifting environment. Application of the dynamic melting inversion method suggests that the degree of partial melting of the SB ranges from 7% to 12%. Unlike large-volume tholeiites, these low-degree transitional basaltic melts may represent the waning stage of plume volcanism during a long-lasting continental breakup.

(3) Based on the new ages of the SB and its relationship with the Yuermeinak diamictite, the Yuermeinak glaciation in Sugetbrak of the northwest Tarim Block should correlate with the Tereekeng glaciation in the Qurugtagh area of the northeast Tarim Block, the Nantuo glaciation in the Yangtze Block and the Elatin glaciation in Australia.

Acknowledgements

We are grateful to anonymous reviewers for their constructive reviews that significantly improved the quality of this paper. We also thank Biao Song for his help in SHRIMP analyses of zircons, Chen Peng, Wei Wei, and Tong Qinlong for field assistance, and Li Huaikun and Wang Yanyang for drawing figures. Ross T. Tucker and Erin Summerlin from Auburn University provided helpful in-house reviews. This study was supported by grants from the National Natural Science Foundation of China (40972126, 41121062).

References

- BGMRED of Xinjiang, 1993. Regional Geology of Xinjiang Uygur Autonomous Region. Geol. Publ. House, Beijing, 841pp (in Chinese with English abstract).
- Bullerud, K., Skjerlie, K.P., Corfu, F., de la Rosa, J., 2006. The 2.40 Ga Ringvassoy mafic dykes, West Troms Basement Complex, Norway: The concluding act of early Palaeoproterozoic continental breakup. *Precambrian Res.* 150, 183-200.
- Chen, Y., Xu, B., Zhan, S., Li, Y.A., 2004. First mid-Neoproterozoic paleomagnetic results from the Tarim Basin (NW China) and their geodynamic implications. *Precambrian Res.* 133, 271-281.
- Chu, X.L., Todt, W., Zhang, Q.R., Chen, F.K., Huang J., 2005. U-Pb zircon age for the Nanhua-Sinian boundary. *Chinese Science Bulletin*, 50 (7): 716-718.
- Compston, W., Williams, I.S., Kirschvink, J.L., Zhang, Z., Ma, G., 1992. Zircon U-Pb ages of early Cambrian time-scale. *J. Geol. Soc.* 149, 171-184.
- Condon, D., Zhu, M., Bowring, S., Wang, W., Yang, A., Jin, Y., 2005. U-Pb ages from the Neoproterozoic Doushantuo Formation. *Chin. Science* 308, 95-98.
- Direen, N., Crawford, A., 2003, Fossil seaward-dipping reflector sequences preserved in southeastern Australia: a 600 Ma volcanic passive margin in eastern Gondwanaland. *Journal of the Geological Society, London.* 160, 2003, 985-990.
- Gao, J.F., Lu, J.J., Lai, M.Y., 2003. Analysis of trace elements in rock samples using HRICP-MS. *Journal of Nanjing University (Natural Sciences)* 39, 844-850 (in Chinese with English abstract).
- Gao, Z., Zhu, C., 1984. Precambrian Geology in Xinjiang, China. Urumqi, pp. 1-151 (in Chinese with English abstract).
- Gao, Z., Qian, J., 1985. Sinian glacial deposits in Xinjiang, Northwest China. *Precambrian Res.* 29,

143-147.

Gao, Z., Wang, W., Peng, C., Li, Y., Xiao, B., 1985. The Sinian System of Xinjiang. Urumqi, pp. 1-173 (in Chinese with English abstract).

Gao, Z., Wang, W., Peng, C., Li, Y., Xiao, B., 1986. The Sinian System on Aksu-Wushi Region, Xinjiang. Urumqi, pp. 1-184 (in Chinese with English abstract).

Hoffman, P.F., Schrag, D.P., 2002. The snowball Earth hypothesis: testing the limits of global change, *Terra Nova* 14, 129-155.

Hoffmann, K.-H., Condon, D.J., Bowring, S.A., Crowley, J.L., 2004. U–Pb zircon date from the Neoproterozoic Ghaub Formation Namibia: constraints on Marinoan glaciation. *Geology* 32, 817–820.

Hoffmann, K.-H., Condon, D.J., Bowring, S.A., Prave, A.R., Fallick, A., 2006. Litho-stratigraphic, carbon (^{13}C) isotope and U–Pb zircon age constraints on early Neoproterozoic (ca. 755 Ma) glaciation in the Gariep Belt, southern Namibia. In: *Proceedings of the Snowball Earth Conference*, July 16-21, 2006, Monte Verita, Ticino, Switzerland, p. 51.

Hu, A.Q., Jahn, B.M., Zhang, G.X., Chen, Y.B., Zhang, Q.F., 2000. Crustal evolution and Phanerozoic crustal growth in northern Xinjiang: Nd isotope evidence, 1. Isotopic characterization of basement rocks. *Tectonophysics* 328, 15–51.

Jefferson, C.W., Parrish, R.R., 1989. Late Proterozoic stratigraphy, U–Pb zircon ages, and rift tectonics, Mackenzie Mountains, northwestern Canada. *Can. J. Earth Sci.* 26, 1784–1801.

Jiang, G., Kennedy, M.J., Christie-Blick, N., 2003. Stable isotopic evidence for methane seeps in Neoproterozoic postglacial cap carbonates. *Nature* 426, 822–826.

Karlstrom, K.E., Bowring, S.A., Dehler, C.M., Knoll, A.H., Porter, S.M., Marais, D.J.D.B., Weil,

- A., Sharp, Z.D., Geissman, J.W., Elrick, M.B., Timmons, J.M., Crossey, L.J., Davidek, K.L., 2000. Chuar Group of the Grand Canyon: Record of breakup of Rodinia, associated change in the global carbon cycle, and ecosystem expansion by 740 Ma. *Geology* 28, 619–622.
- Kennedy, M.J., Runnegar, Kheraskova, T. N., Bush, V. A., Didenko, A. N., Samygin, S. G., 2010. Breakup of Rodinia and Early Stages of Evolution of the Paleasian Ocean. *Geotectonics* 44, 3-24.
- Kou, X., Wang, Y., Wei, W., He, J., Xu, B., 2008. The Neoproterozoic Altungol and Huangyanggou formations in Tarim plate: recognized Newly glaciation and interglaciation. *Acta Petrologica Sinica* 24, 2863-2869 (in Chinese with English abstract).
- Li, X.H., Li, Z.X., Zhou, H.W., Liu, Y., Kinny, P.D., 2002. U–Pb zircon geochronology, geochemistry and Nd isotopic study of Neoproterozoic bimodal volcanic rocks in the Kangdian Rift of South China: implications for the initial rifting of Rodinia. *Precambrian Res.* 113, 135-154.
- Li, X.H., Li, Z.X., Ge, W., Zhou, H., Li, W., Liu, Y., Wingate, M.T.D., 2003. Neoproterozoic granitoids in South China: crustal melting above a mantle plume at ca. 825 Ma? *Precambrian Res.* 122, 45-84.
- Li, X.H., Li, Z.X., Wingate, M.T.D., Chung, S.L., Liu, Y., Lin, G.C., Li, W.X., 2006. Geochemistry of the 755 Ma Mundine Well dyke swarm, northwestern Australia: part of a Neoproterozoic mantle superplume beneath Rodinia? *Precambrian Res.* 146, 1-15.
- Li, X.H., Zhu, W.G., Zhong, H., Wang, X.C., He, D.F., Bai, Z.J., Feng, L., 2010. The Tongdepicritic dikes in the Western Yangtze Block: evidence for ca 800-Ma mantle plume magmatism in south China during the breakup of Rodinia. *J. of Geol.* 118 509-522.

- Li, Z.X., Zhang, L., Powell, C.M., 1996. Positions of the East Asian cratons in the Neoproterozoic supercontinent Rodinia, *Aust. J. Earth Sci.* 43, 593-604.
- Li, Z.X., Li, X.H., Kinny, P.D., Wang, J., 1999. The breakup of Rodinia: Did it start with a mantle plume beneath South China? *Earth Planet. Sci. Lett.* 173, 171-181.
- Li, Z.X., Powell, C.M., 2001. An outline of the palaeogeographic evolution of the Australasian region since the beginning of the Neoproterozoic. *Earth Sci. Rev.* 53, 237-277.
- Li, Z.X., Li, X.H., Kinny, P.D., Wang, J., Zhang, S., Zhou, H., 2003. Geochronology of Neoproterozoic syn-rift magmatism in the Yangtze Craton, South China and correlations with other continents: evidence for a mantle superplume that broke up Rodinia. *Precambrian Res.* 122, 85-110.
- Li, Z.X., Bogdanova, S.V., et al. 2008. Assembly, configuration, and break-up history of Rodinia: A synthesis. *Precambrian Research*, 160, 179–210.
- Ling, W., Gao, S., Zhang, B., Li, H., Liu, Y., Cheng, J., 2003. Neoproterozoic tectonic evolution of the northwestern Yangtze craton, South China: implications for amalgamation and break-up of the Rodinia Supercontinent. *Precambrian Res.* 122, 111-140.
- Liou, J.G., Graham, S.A., Mayuyama, S., Wang, X., Xiao, X., Carroll, A. R., Chu, J., Feng, Y., Hendrix, M.S., Liang, Y., Mcknight, C.L., Yang, Y., Wang, Z., Zhao, M., Zhu. B., 1989. Proterozoic blueschist belt in western China: Best-documented Precambrian blueschists in the world. *Geology* 17, 1127–1131.
- Liou, J.G., Maruyama, S., Wang, X., Graham, S., 1990. Precambrian blueschist terranes of the world. *Tectonophysics* 181, 97–111.
- Liou, J.G., Graham, S.A., Maruyama, S., Zhang, R.Y., 1996. Characteristics and

- tectonic significance of the Late Proterozoic Aksu blueschists and diabasic dikes, Northwest Xinjiang, China. *International Geological Review* 38, 228–244.
- Long, X.P., Yuan, C., Sun, M., Kröner, A., Zhao, G.C., Wilde, S., Hu, A., 2011. Reworking of the Tarim Craton by underplating of mantle plume-derived magmas: Evidence from Neoproterozoic granitoids in the Kulu ketage area, NW China. *Precambrian Res.* 187, 1-14.
- Lu, S., Li, H., Zhang, C., Niu, G., 2008. Geological and geochronological evidence for the Precambrian evolution of the Tarim Craton and surrounding continental fragments. *Precambrian Res.* 160, 94-107.
- Ludwig, K.R., 1999. Using Isoplot/EX, version 2, a geochronological Toolkit for Microsoft Excel. Berkeley Geochronological Center Special Publication 1a, 47.
- Ludwig, K.R., 2001. Squid 1.02: A user manual. Berkeley Geochronological Center Special Publication 2, 19.
- Macdonald, F.A., Schmitz, M.D., Crowley, J.L., Roots, C.F., Jones, D.S., Maloof, A.C., Strauss, J.V., Cohen, P.A., Johnston, D.T., Schrag, D.P., 2010. Calibrating the Cryogenian. *Science* 327, 1241-1243.
- Meschede, M., 1986. A method of discriminating between different types of mid-ocean ridge basalts and continental tholeiites with the Nb-Zr-Y diagram. *Chem. Geol.* 56, 207-218.
- Nakajima, T., Maruyama, S., Uchiumi, S., Liou, J.G., Wang, X., Xiao, X., Graham, A., 1990. Evidence for late Proterozoic subduction from 700-Myr-old blueschists in China. *Nature* 346, 263-265.
- Pearce, J.A., Cann, J.R., 1973. Tectonic setting of basic volcanic rocks determined using trace element analyses. *Earth Planet. Sci. Lett.* 19, 290-300.

- Ross, G.M., Villeneuve, M.E., 1997. U–Pb geochronology of stranger stones in Neoproterozoic diamictites, Canadian Cordillera: implications for provenance and age of deposition. *Geological Survey of Canada, Current Research 1997-F*, 141–155.
- Shu, L.S., Deng, X.L., Zhu, W.B., Ma, D.S., Xiao, W.J., 2011. Precambrian tectonic evolution of the Tarim Block, NW China: New geochronological insights from the Quruqtagh domain. *J. Asian Earth Science* 42, 774-790.
- Turner, S., 2010. Sedimentary record of Late Neoproterozoic rifting in the NW Tarim basin, China. *Precambrian Res.* 181, 85-96
- Veevers, J., 2000. Billion-year Earth History of Australia and its Neighbours in Gondwanaland. GEMOD Press, Sydney
- Veevers, J.J., Walter, M.R., Scheibner, E., 1997. Neoproterozoic tectonics of Australia-Antarctica and Laurentia and the 560 Ma birth of the Pacific ocean reflect the 400 m.y. Pangean supercycle. *J. Geol.* 105, 225-242.
- Wang, F., Wang, B., Shu, L., 2010a. Continental tholeiitic basalt of the Aksu area (NW China) and its implication for the Neoproterozoic rifting in the northern Tarim. *Acta Petrologica Sinica* 26, 547-558. (in Chinese with English abstract).
- Wang, Y., He, J., Wei, W., Xu, B., 2010b. Study on the late Proterozoic sedimentary facies and sequence stratigraphy in Aksu area, Xinjiang. *Acta Petrologica Sinica* 26, 2519-2528 (in Chinese with English abstract).
- Williams, I.S., Claesson, S., 1987. Isotope evidence for the Precambrian province and Caledonian metamorphism of high grade paragneiss from the SveNappes, Scandinavian Caledonides, II. Ion microprobe zircon U-Th-Pb. *Contrib. Mineral. Petrol.* 97, 205-217.

- Winchester, J.A., Floyd, P.A., 1977. Geochemical discrimination of different magma series and their differentiation products using immobile elements. *Chem. Geol.* 20, 325-343.
- Wingate, M.T.D., Campbell, I.H., Compston, W., Gibson, G.M., 1998. Ion microprobe U-Pb ages for Neoproterozoic basaltic magmatism in south-central Australia and implications for the breakup of Rodinia. *Precambrian Res.* 87, 135-159.
- Xiao, S., Bao, H., Wang, H., Kaufman, A.J., Zhou, C., Li, G., Yuan, X., Ling, H., 2004. The Neoproterozoic Quruqtagh Group in eastern Chinese Tianshan: evidence for a post-Marinoan glaciation. *Precambrian Res.* 130, 1-26.
- Xu, B., Jian, P., Zheng, H., Zou, H., Zhang, L., Liu, D., 2005. U-Pb zircon geochronology and geochemistry of Neoproterozoic volcanic rocks in the Tarim Block of Northwest China: implications for the breakup of Rodinia supercontinent and Neoproterozoic glaciations. *Precambrian Res.* 136, 107-123.
- Xu, B., Kou, X., Song, B., Wei, W., Wang, Y., 2008. SHRIMP dating of the upper Proterozoic volcanic rocks in the Tarim plate and constraints on the Neoproterozoic glaciations. *Acta Petrologica Sinica* 24, 2857-2862 (in Chinese with English abstract).
- Xu, B., Xiao, S., Zou, H., Chen, Y., Li, Z., Song, B., Liu, D., Zhou, C., Yuan, X., 2009. SHRIMP zircon U-Pb age constraints on Neoproterozoic Quruqtagh diamictites in NW China. *Precambrian Res.* 168, 247-258.
- Yin, C., Liu, D., Gao, L., Wang, Z., Xing, Y., Jian, P., Shi, Y., 2003. Lower boundary age of the Nanhua System and the Gucheng glacial stage: evidence from SHRIMP II dating. *Chin. Sci. Bull.* 48 (16), 1657-1662.

- Zhan, S., Chen, Y., Xu, B., Wang, B., Faure, M., 2007. Late Neoproterozoic paleomagnetic results from the Sugetbrak Formation of the Aksu area, Tarim basin (NW China) and their implications to paleogeographic reconstructions and the snowball Earth hypothesis. *Precambrian Res.* 154, 143-158.
- Zhang, B., Zhu, W., Jahn, B., Shu, L., Zhang, Z., Su, J., 2010. Subducted Precambrian oceanic crust: geochemical and Sr–Nd isotopic evidence from metabasalts of the Aksu blueschist, NW China. *Journal of the Geological Society, London*, 167, 1161–1170.
- Zhang, C., Li, Z., Li, X., Ye, H., 2009. Neoproterozoic mafic dyke swarms at the northern margin of the Tarim Block, NW China: Age, geochemistry, petrogenesis and tectonic implications. *Journal of Asian Earth Sciences* 35, 167–179.
- Zhang, C., Yang, D., Wang, H., Takahashi, Y., Ye, H., 2011. Neoproterozoic mafic-ultramafic layered intrusion in Quruqtagh of northeastern Tarim Block, NW China: Two phases of mafic igneous activity with different mantle sources. *Gondwana Research* 19, 177–190.
- Zhang, L., Jiang, W., Wei, C., Dong, S., 1999. Discovery of deerite from the Aksu Precambrian blueschist terrane and its geological significance. *Science in China (series D)* 42, 233-239.
- Zhang, S., Jiang, G., Zhang, J., Song, B., Kennedy, M.J., Christie-Blick, N., 2005. U–Pb sensitive high-resolution ion microprobe ages from the Doushantuo Formation in south China: constraints on late Neoproterozoic glaciations. *Geology* 33, 473–476.
- Zhang, Z. C., Kang, J. L., Kusky, T., Santosh, M., Huang, H., Zhang, D. Y. and Zhu, J., 2012. Geochronology, geochemistry and petrogenesis of Neoproterozoic basalts from Sugetbrak, northwest Tarim block, China: Implications for the onset of Rodinia supercontinent breakup. *Precambrian Research* 220-221, 158-176.

Zhou, C., Tucker, R., Xiao, S., Peng, Z., Yuan, X., Chen, Z., 2004. New constraints on the ages of Neoproterozoic glaciations in South China. *Geology* 32, 437–440.

Zhu, W., Zheng, B., Shu, L., Ma, D., Wu, H., Li, Y., Huang, W., Yu, J., 2011. Neoproterozoic tectonic evolution of the Precambrian Aksu blueschist terrane, northwestern Tarim, China: Insights from LA-ICP-MS zircon U–Pb ages and geochemical data. *Precambrian Res.* 185, 215–230.

Zou, H. B., Zindler, A., 1996. Constraints on the degree of dynamic partial melting and source composition using concentration ratios in magmas. *Geochimica et Cosmochimica Acta* 60, 711–717.

Zou, H. B., 1998. Trace element fractionation during modal and nonmodal dynamic melting and open-system melting: A mathematical treatment. *Geochimica et Cosmochimica Acta* 62, 1937–1945.

Zou, H. B., Zindler, A., Xu, X. S. and Qi, Q., 2000. Major, trace element, and Nd, Sr and Pb isotope studies of Cenozoic basalts in SE China: mantle sources, regional variations and tectonic significance. *Chemical Geology* 171, 33–47.

Figure Captions

Fig. 1. (A): Tectonic location of the Tarim Block in China; (B): Geological map of the Tarim Block, West China, showing the distribution of Neoproterozoic and the study area. Legend—PH: Phanerozoic rocks; NP: Neoproterozoic rocks; MP: Mesoproterozoic rocks; PP: Palaeoproterozoic rocks; AR: Archaean rocks; NPG: early Neoproterozoic granitoids; F: faults; IF: inferred faults; Tillite: Neoproterozoic tillite; Q: Quaternary desert and sedimentary deposits (modified after Lu, et al., 2008); (C): Geological map of the Aksu area (modified after Gao, et al., 1985; Turner, 2010).

Fig. 2. (A): Geological map of the Sugetbrak area and sample positions (modified after BGMRED of Xinjiang, 1993); (B): the Neoproterozoic stratigraphic column of the Sugetbrak area; (C): Photograph of the Neoproterozoic succession in the Sugetbrak area. Notice the positions of SB sample 05822.

Fig.3. Photographs of the SB and sedimentary rocks of the Sugetbrak Formation. (A): largeherringbone and conformity relationships between the SB and underlying sandstone; (B):columnar joints of the SB; (C): Continuous distribution of the SB on the south limb of a syncline; (D): pillow lava in the SB; (E): conformity relationship between the SB and overlying red sandstones;(F): ripple bedding in red sandstone of the Lower member of the Sugetbrak Fm.

Fig. 4. A: Cathodoluminescence images of zircons from the SB. Notice the zircons can be divided into 3 groups according to their sizes; B: Concordia plot of zircons from sample 05822 of the SB;
C: Concordia plot of zircons from sample 05823 of the SB.

Fig.5. A: Zr/TiO₂ – Nb/Y diagram (Winchester and Floyd, 1977); B: Nb/Y – Zr/(P₂O₅*10000)diagram (Floyd and Winchester, 1975)

Fig. 6. A: REE diagram of the SB; B: Trace element spider diagram of the SB.

Fig. 7. A: Ti-Zr-Y diagram (Pearce and Cann, 1973); B: Nb-Zr-Y diagram (Meschede, 1986)

Fig. 8. Correlation of the Neoproterozoic between the southwest Aksu, Wushi and Sugetbrak sections in the northwest Tarim Block.

Fig. 9. Correlation of Neoproterozoic glaciations between the northeast Tarim, northwest Tarim and Yangtze Blocks. Data from: Yin et al., 2003; Hoffmann et al., 2004; Zhou et al., 2004; Chu et al., 2005; Condon et al., 2005; Zhang et al., 2005; Kendall et al., 2006; Xu et al., 2009.

Table 1. SHRIMP zircon U-Pb data for the Sugetbrak basalts in Sugetbrak area, northwest Tarim Block

Spot	U (ppm)	Th (ppm)	$^{232}\text{Th}/^{238}\text{U}$	$^{206}\text{Pb}_c$	$^{206}\text{Pb}^*$	$^{206}\text{Pb}/^{238}\text{U}$ Age	$^{207}\text{Pb}/^{206}\text{Pb}$
22-1-1.1	246	147	0.62	0.13	28.9	825.4 ± 8.9	849
22-1-2.1	287	179	0.64	0.30	33.0	808.0 ± 8.4	808
22-1-3.1	355	412	1.20	0.16	37.3	743.4 ± 7.6	737
22-1-4.1	451	209	0.48	0.14	49.6	774.6 ± 7.9	771
22-1-5.1	180	205	1.17	0.26	18.4	722.2 ± 8.1	671
22-1-6.1	159	146	0.95	0.27	17.5	776.1 ± 8.8	779
22-1-7.1	240	164	0.71	0.63	20.9	617.3 ± 6.8	641
22-1-8.1	58	63	1.13	0.85	6.10	744 ±11	797
22-1-9.1	960	536	0.58	2.44	104	750.8 ± 7.3	774
2-1-10.1	171	132	0.80	0.25	19.5	804.2 ± 8.8	825
2-1-11.1	517	425	0.85	0.75	64.0	861.9 ± 8.7	808
822-12.1	63	67	1.11	0.36	6.96	780 ±10	639
822-13.1	155	104	0.69	16.79	18.6	707 ±16	590
2-1A-1.1	72	83	1.19	0.30	7.57	743.3 ±7.5	833
2-1A-2.1	284	83	0.30	0.06	32.5	805.9 ±4.2	820
2-1A-3.1	71	82	1.19	0.67	7.78	773.0 ±8.0	703
2-1A-4.1	87	89	1.06	1.57	9.48	758.9 ±7.6	712
2-1A-5.1	442	111	0.26	0.13	38.0	614.9 ±2.6	671
2-1A-6.1	361	416	1.19	0.24	40.6	790.4 ±3.7	816
2-1A-7.1	832	305	0.38	0.51	103	863.6 ±3.2	841
3-11-1.1	233	151	0.67	0.48	27.3	821.2 ± 9.5	760
3-11-2.1	1102	816	0.77	0.69	95.7	616.6 ± 6.6	694
3-11-3.1	568	741	1.35	0.32	54.1	676.2 ± 7.5	657
3-11-4.1	415	200	0.50	0.12	110	1,735 ±17	1,755.6
3-11-5.1	623	949	1.58	0.22	53.4	612.3 ± 6.5	663
3-11-6.1	762	558	0.76	0.37	73.7	685.6 ± 7.3	689
3-11-7.1	140	216	1.59	0.92	16.9	839 ±11	698
3-11-8.1	588	261	0.46	0.20	57.3	691.4 ± 7.3	778
3-11-9.1	461	184	0.41	0.15	52.8	806.8 ± 8.8	801

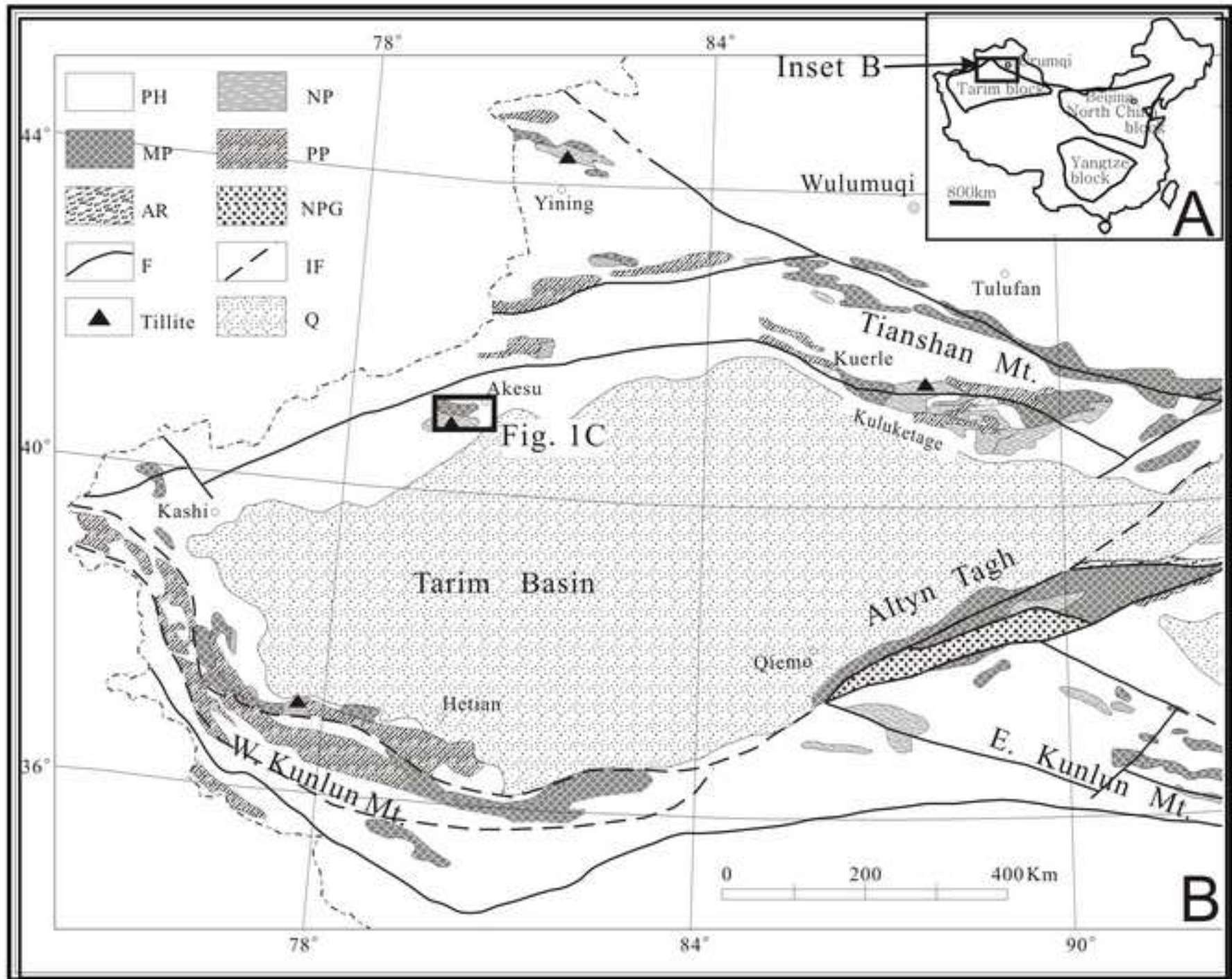
Errors are 1-sigma; Pb_c and Pb^* indicate the common and radiogenic portions, respectively. Error in Standard calibration was 0.20% (not included in above errors but required when: (1) Common Pb corrected using measured ^{204}Pb . (2) Common Pb corrected by assuming ^{206}Pb . (3) Common Pb corrected by assuming $^{206}\text{Pb}/^{238}\text{U}$ - $^{208}\text{Pb}/^{232}\text{Th}$ age-concordance.

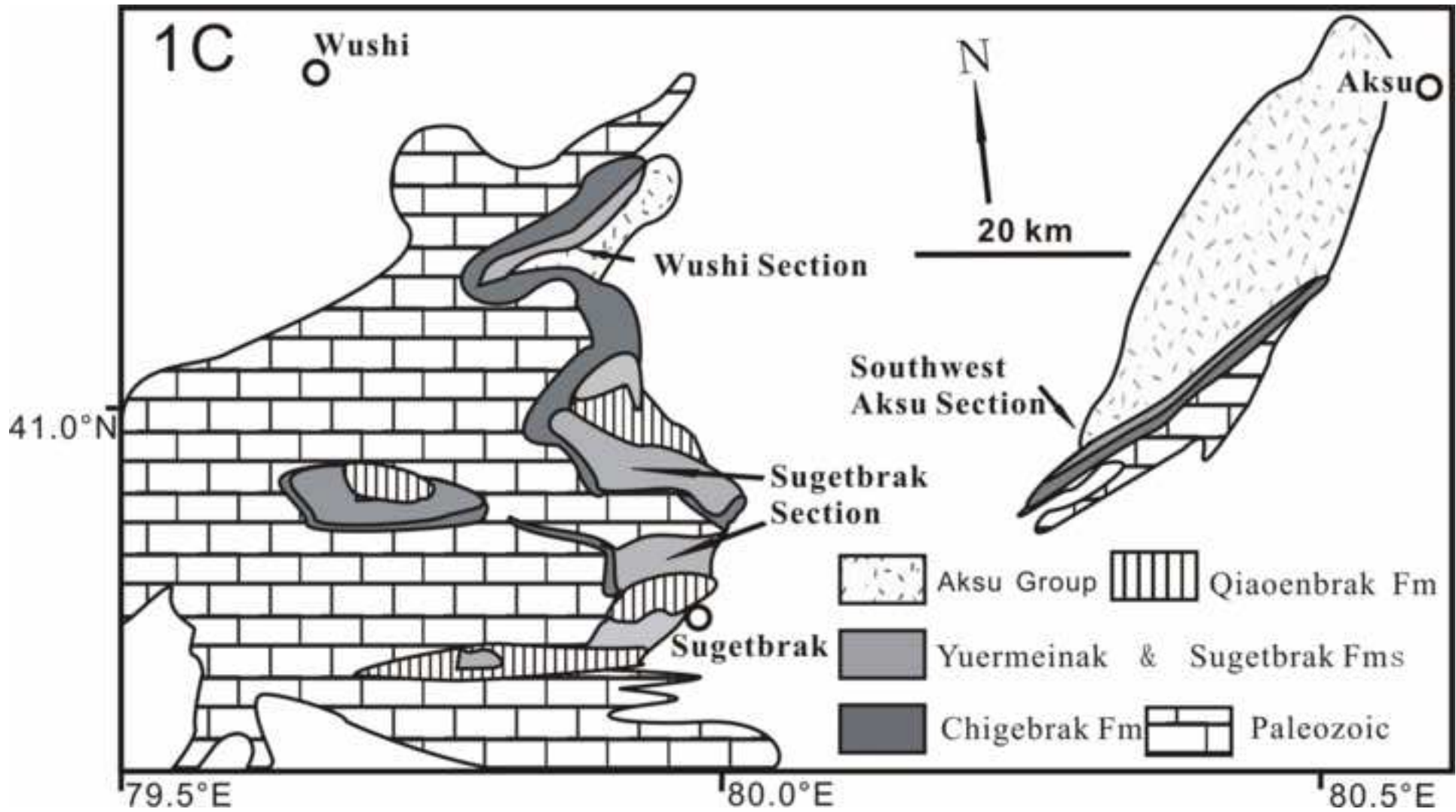
Table 2 Major and trace element abundances for the Sugetbrak basalts in Sugetbrak area, west Tarim Bl

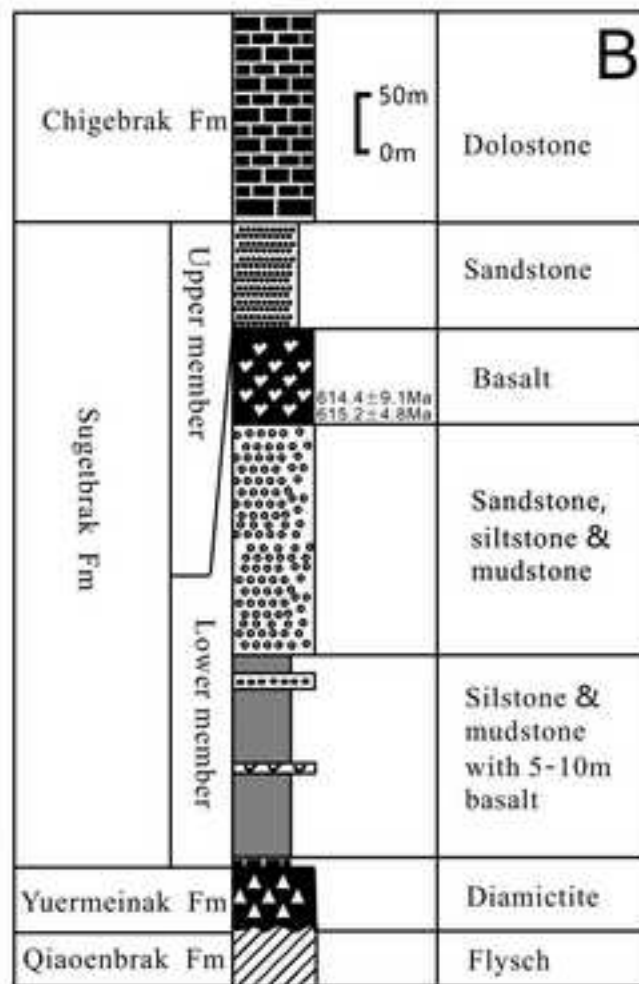
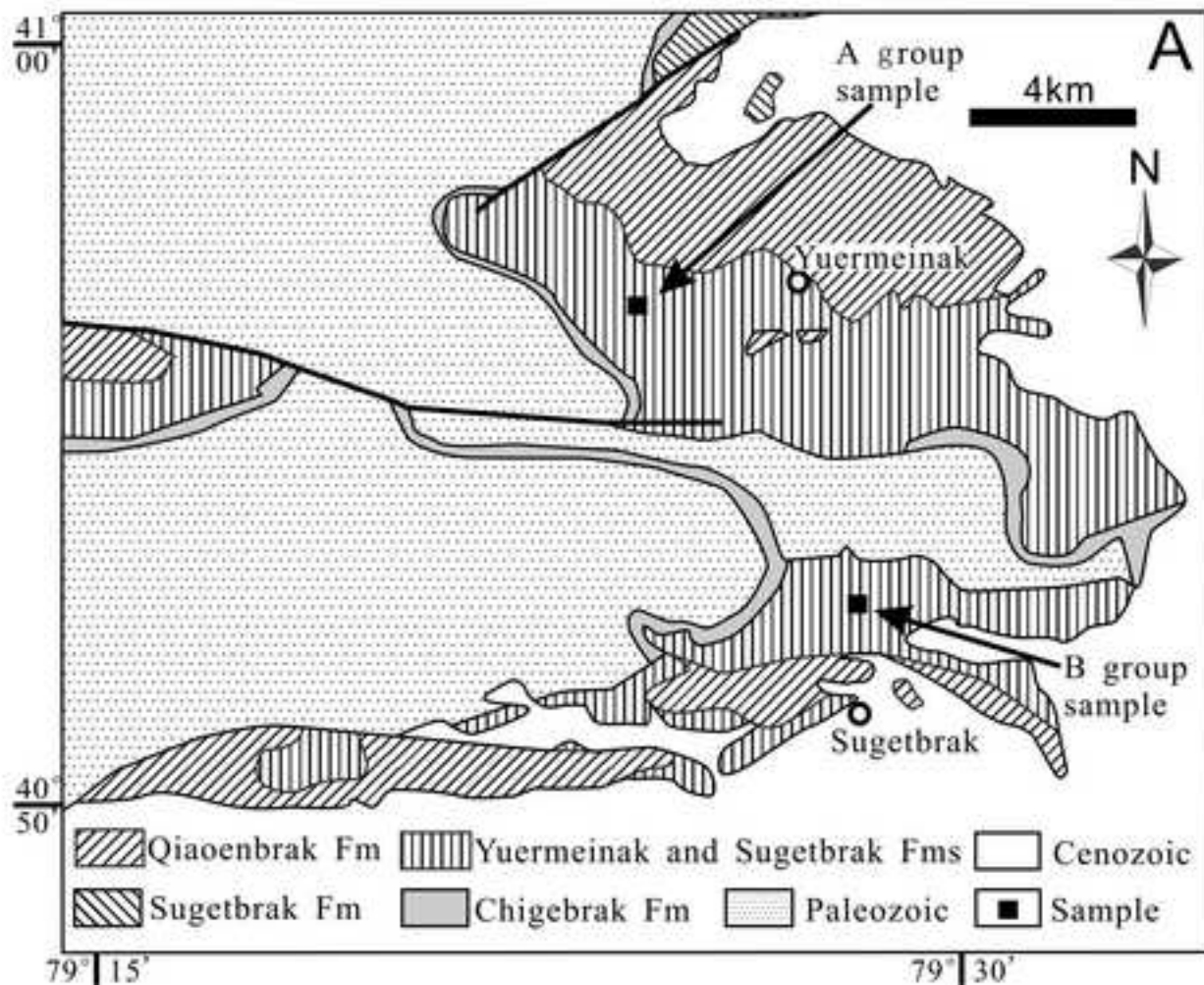
Sample	831S41	831S51	830S2	83156	83158	83160	83161	83163
SiO ₂	44.35	43.45	45.40	44.38	45.47	45.44	46.81	44.37
TiO ₂	4.002	3.494	3.763	3.124	2.865	2.215	2.216	2.489
Al ₂ O ₃	13.91	14.91	13.92	14.9	15.32	16.95	16.73	17.73
MgO	4.52	5.11	5.3	5.88	5.33	5.29	5.19	6.44
Fe ₂ O ₃	16.47	13.76	16.46	16.34	15.38	13.22	13.5	12.52
MnO	0.241	0.643	0.251	0.236	0.2	0.131	0.125	0.16
CaO	8.00	8.21	8.00	5.45	7.30	7.18	5.98	4.84
K ₂ O	0.28	0.62	0.66	1.23	1.18	1.41	1.67	0.59
Na ₂ O	4.01	3.16	2.93	3.3	2.48	3.36	3.59	3.75
P ₂ O ₅	0.66	0.598	0.635	0.481	0.457	0.452	0.462	0.468
LOI	3.57	6.06	2.72	4.8	4.07	4.45	3.83	6.9
Total	100.01	100.02	100.04	100.13	100.05	100.09	100.11	100.26
Ti	24519	21911	23322	19024	17451	13702	13690	15193
Rb	6.56	12.68	10.31	17.23	17.42	22.93	29.61	8.86
Sr	718	474	474	342	383	464	442	335
Y	37.2	33.2	35.2	33.9	33.3	26.3	26.9	27.6
Zr	200	183	192	190	188	150	152	158
Nb	24.63	22.58	23.23	21.49	21.07	16.24	16.27	17.64
Cs	0.16	0.41	0.28	0.15	0.07	0.11	0.12	0.30
Ba	121	292	444	831	889	696	705	327
Hf	4.79	4.38	4.80	4.55	4.47	3.71	3.68	3.87
Ta	1.60	1.42	1.54	1.38	1.35	1.03	1.02	1.11
Pb	4.02	14.93	4.01	1.70	2.67	3.46	3.58	6.64
Th	2.99	2.72	2.81	2.16	2.11	1.75	1.77	1.83
U	0.68	0.66	0.62	1.27	0.54	0.41	0.40	0.45

Table2 (continued)

Sample	831S41	831S51	830S2	83156	83158	83160	83161	83163
La	37.42	33.39	34.29	28.31	26.41	26.43	26.29	26.38
Ce	74.41	67.07	68.73	55.70	52.86	51.41	51.42	51.79
Pr	9.22	8.53	8.81	7.31	7.17	6.65	6.60	6.84
Nd	39.80	36.03	36.61	32.03	30.63	27.98	28.56	29.78
Sm	8.08	7.36	7.65	6.66	6.59	5.80	5.80	6.17
Eu	2.66	2.46	2.52	2.32	2.30	2.21	2.15	2.40
Gd	8.62	7.95	8.27	7.32	7.09	6.04	6.28	6.41
Tb	1.10	1.00	1.06	0.98	0.93	0.80	0.78	0.81
Dy	7.01	6.40	6.65	6.37	6.02	4.99	5.15	5.17
Ho	1.44	1.30	1.36	1.30	1.24	1.04	1.03	1.06
Er	3.74	3.45	3.63	3.31	3.37	2.77	2.76	2.86
Tm	0.51	0.46	0.48	0.46	0.45	0.36	0.36	0.38
Yb	2.81	2.68	2.76	2.69	2.68	2.11	2.19	2.19
Lu	0.44	0.42	0.43	0.45	0.42	0.33	0.34	0.34

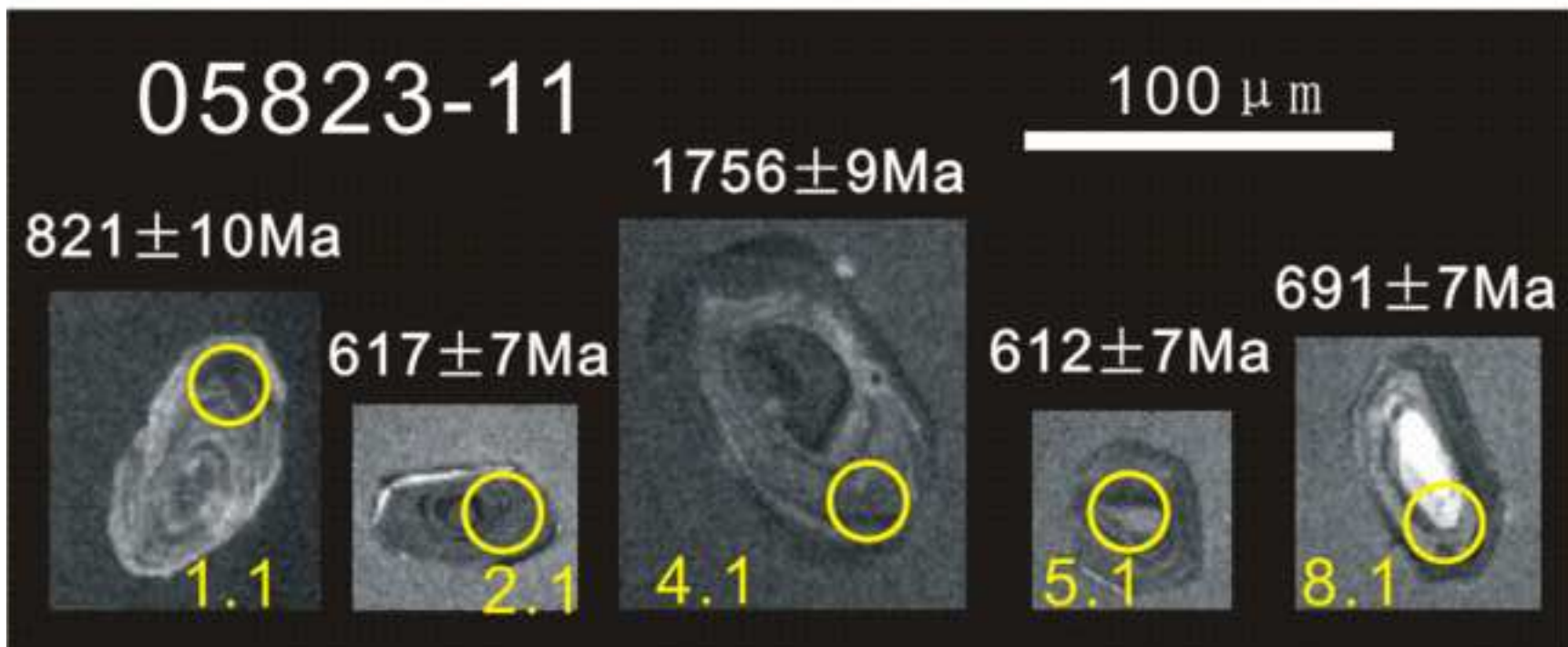
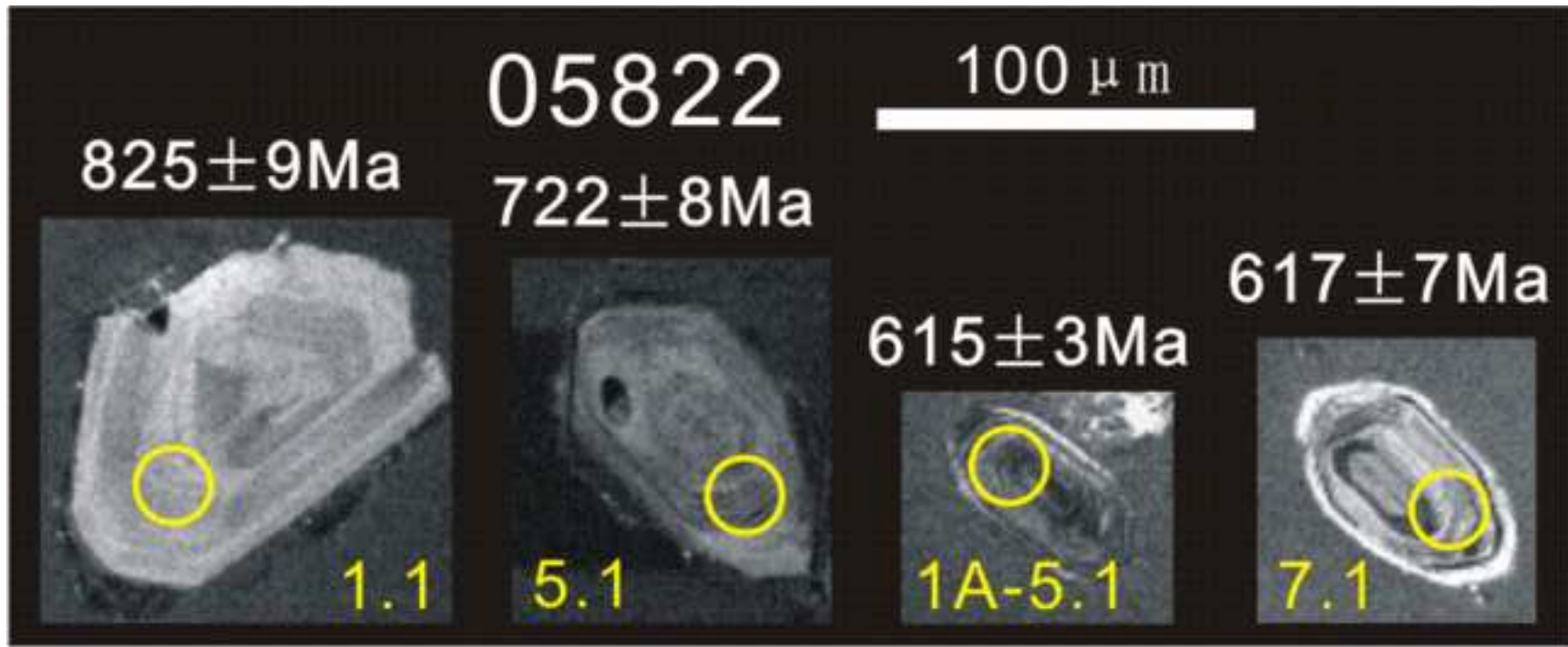












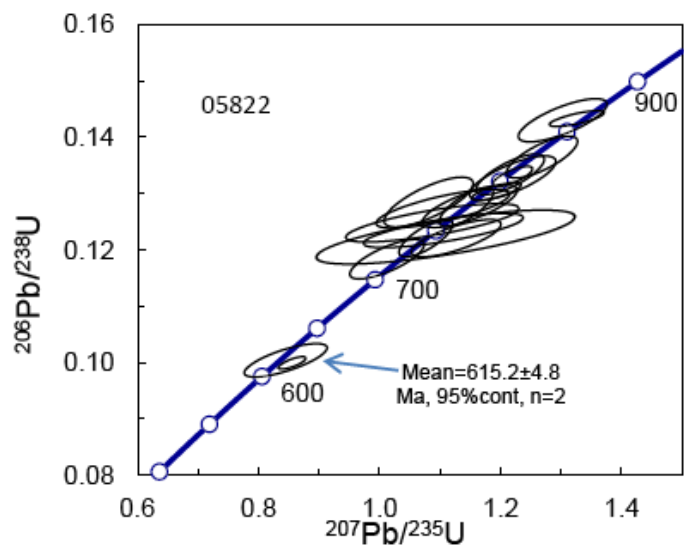


Fig.4B

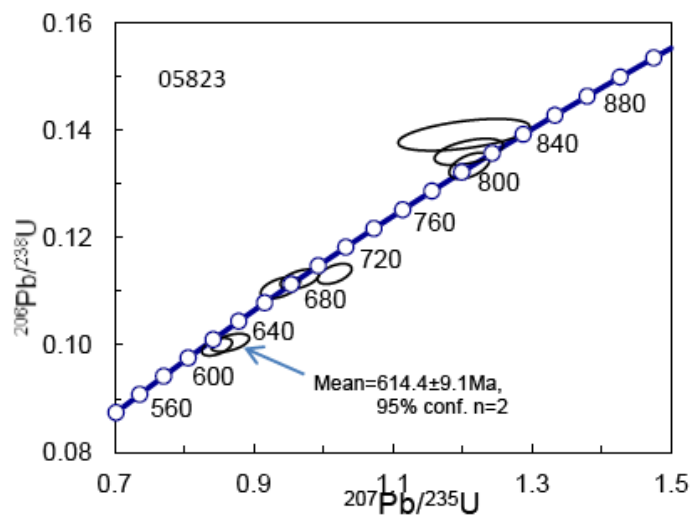


Fig.4C

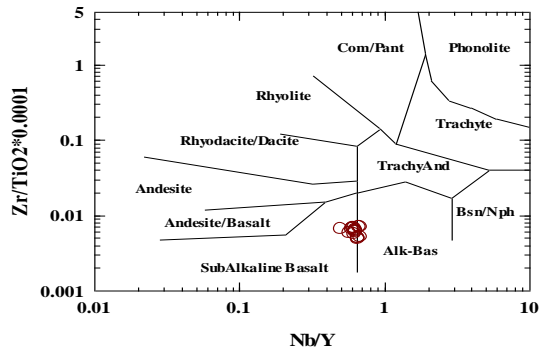


Fig.5A

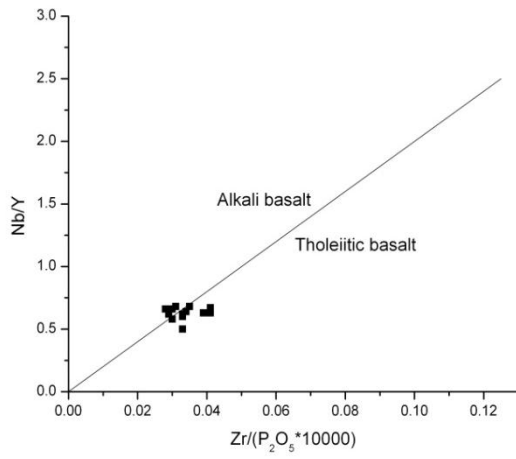


Fig.5B

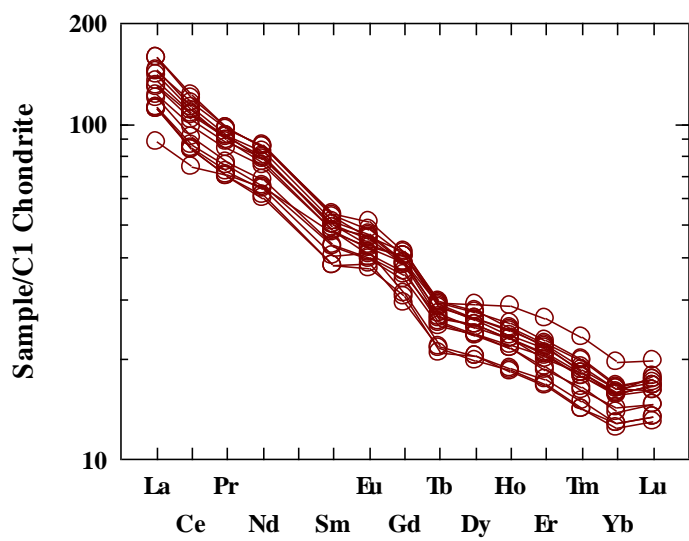


Fig.6A

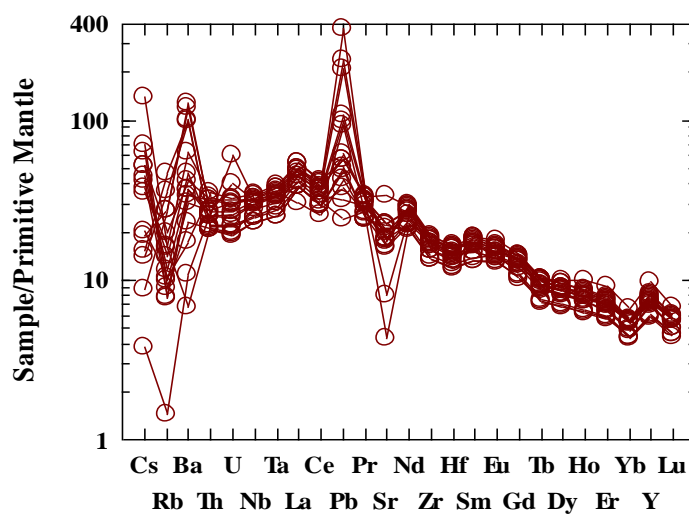


Fig.6B

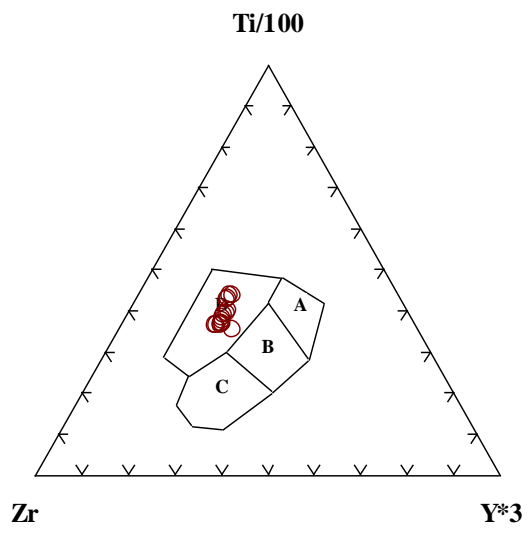


Fig.7A

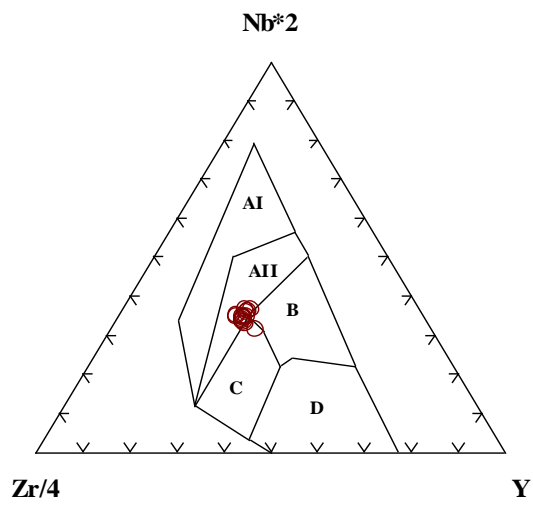


Fig.7B

Sugetbrak section

Southwest Aksu section

Wushi section

